THE JOURNAL OF BIOLOGICAL CHEMISTRY VOL. 281, NO. 51, pp. 39300–39307, December 22, 2006

Molecular Determinants for G Protein $\beta\gamma$ Modulation of Ionotropic Glycine Receptors*

Received for publication, August 29, 2006, and in revised form, October 4, 2006 Published, JBC Papers in Press, October 12, 2006, DOI 10.1074/jbc.M608272200

Gonzalo E. Yevenes[‡], Gustavo Moraga-Cid[‡], Leonardo Guzmán[‡], Svenja Haeger[§], Laerte Oliveira[¶], Juan Olate[‖], Günther Schmalzing[§], and Luis G. Aguayo[‡1]

From the [‡]Laboratory of Neurophysiology, Department of Physiology, University of Concepción, Concepción, Chile, the [§]Department of Molecular Pharmacology, Medical School of the Technical University of Aachen, Aachen, Germany, the [¶]Escola Paulista de Medicina, Universidade Federal de São Paulo, São Paulo, Brazil, and the [‖]Laboratory of Molecular Genetics, Department of Biochemistry and Molecular Biology, University of Concepción, Concepción, Chile

The ligand-gated ion channel superfamily plays a critical role in neuronal excitability. The functions of glycine receptor (GlyR) and nicotinic acetylcholine receptor are modulated by G protein $\beta\gamma$ subunits. The molecular determinants for this functional modulation, however, are still unknown. Studying mutant receptors, we identified two basic amino acid motifs within the large intracellular loop of the GlyR α_1 subunit that are critical for binding and functional modulation by G$\beta\gamma$. Mutations within these sequences demonstrated that all of the residues detected are important for G$\beta\gamma$ modulation, although both motifs are necessary for full binding. Molecular modeling predicts that these sites are α-helixes near transmembrane domains 3 and 4, near to the lipid bilayer and highly electropositive. Our results demonstrate for the first time the sites for G protein $\beta\gamma$ subunit modulation on GlyRs and provide a new framework regarding the ligand-gated ion channel superfamily regulation by intracellular signaling.

The ionotropic glycine receptors (GlyRs)[2] are members of the ligand-gated ion receptor superfamily, which includes inhibitory γ-aminobutyric acid type A receptors and excitatory nAChR and 5-HT_3 receptors. These homologous receptors mediate fast synaptic transmission in the central nervous system (1, 2). Inhibitory GlyRs are critical for the control of excitability in the mammalian spinal cord and brain stem. Binding of glycine to the extracellular region induces a rapid increase in Cl^- ion conductance, generating a hyperpolarization of the cell membrane (3–5). In neurons, the inhibitory action of GlyRs regulate several important physiological functions, like pain transmission, respiratory rhythms, motor coordination, and development (3–7). Like all members of the LGIC superfamily, GlyRs are pentamers composed of five subunits in which each subunit possesses four transmembrane domains arranged to form the ion pore. In this structure, the individual subunits provide extracellular and intracellular domains that play roles in ligand binding and intracellular modulation, respectively (1–3, 5).

The function of GlyRs can be effectively modulated by extracellularly acting compounds like strychnine, picrotoxin, zinc ions, and ethanol (3–5, 8, 9). Furthermore, the receptor can also be modulated by intracellular signaling. One of the most studied and recognized pathways involved in regulation of ligand-gated ion channel function are phosphorylation processes through protein kinases. Indeed, GlyR and other members of the LGIC superfamily are modulated by activation of cAMP-dependent kinases and protein kinase C (10). This involves specific serine residues in the loop between transmembrane domains 3 and 4 (6, 10–14). On the other hand, recent reports have shown that the activity of GlyRs and nAChRs can be modulated by G protein $\beta\gamma$ subunits in a phosphorylation-independent manner (15, 16). In both cases, activation of G proteins, using nonhydrolyzable GTP analogs or by application of purified G$\beta\gamma$ dimers, generates a strong enhancement in the agonist-evoked current, related to a shift to the left in the agonist concentration-response curve and an increased open channel probability (15, 16). However, the molecular determinants involved for this modulation are unresolved.

On the other hand, some molecular characteristics for binding and modulation of G$\beta\gamma$ to other effector proteins are better understood (17–19). In fact, previous studies implicated the presence of basic amino acids, such as lysine and arginine, in the modulation of voltage-gated calcium channels, phospholipase Cβ, and β-adrenergic receptor kinases (20–23). For example, mutations in basic residues reduced G$\beta\gamma$ binding to β-adrenergic receptor kinase 1 and phospholipase Cβ3 (21, 22). Furthermore, similar results were obtained with mutations in the N-terminal region and in the cytoplasmic linker between the first and second transmembrane repeats of voltage-gated calcium channels (19, 20, 23).

In the present study, we have examined the molecular determinants for G protein modulation of the human GlyR α_1 subunit. The present study shows that most of the large intracellular loop is not involved in the modulation. We identified two basic amino acid motifs within the loop of the GlyR as critical for binding and functional modulation by G$\beta\gamma$ dimers. Acidic

* This work was supported by the National Institute on Alcohol Abuse and Alcoholism Grant RO1 AA15150-01, FONDECYT Grant 1020475, CONICYT Grant AT-4040102, funds from the Andes Foundation, and Deutsche Forschungsgemeinschaft Grants Schm536/4-l and 4-2. The costs of publication of this article were defrayed in part by the payment of page charges. This article must therefore be hereby marked "*advertisement*" in accordance with 18 U.S.C. Section 1734 solely to indicate this fact.

[1] To whom correspondence should be addressed: Dept. of Physiology, University of Concepción, P.O. Box 160-C, Concepción, Chile. Tel.: 56-41-2203380; Fax: 56-41-2245975; E-mail: laguayo@udec.cl.

[2] The abbreviations used are: GlyR, glycine receptor; LGIC, ligand-gated ion channel; nAChR, nicotinic acetylcholine receptor; GTPγS, guanosine 5′-*O*-(3-thiotriphosphate); GST, glutathione *S*-transferase; ANOVA, analysis of variance; TM, transmembrane domain; GIRK, G protein-gated inwardly rectifying potassium channel; 5 HT_3, 5 hydroxytryptamine type 3.

residues, on the other hand, are not important for this regulation. These results provide novel information about the Gβγ modulatory sites in the GlyR, a member of the LGIC superfamily, and also demonstrate a new role for specific residues in the intracellular loop for the GlyR function.

EXPERIMENTAL PROCEDURES

cDNA Constructs—The cDNA construct encoding the human glycine receptor α_1 subunit with a C-terminal hexahistidyl tag has been described previously (25). This construct was first subcloned in a pCI vector (Promega) for expression in HEK 293 cells. Mutations were inserted using the QuikChange™ site-directed mutagenesis kit (Stratagene). All of the constructions were confirmed by sequencing. The glycine receptor amino acids were numbered according to their position in the mature protein sequence. pEYFP-Gβ_1 and pECFP-Gγ_2 expression vectors were kindly provided by Stephen R. Ikeda (National Institutes of Health) (27). G protein β_1-FLAG and G protein γ_2 were purchased from UMR cDNA resource center.

Cell Culture and Transfection—HEK 293 cells were cultured using standard methodologies. HEK 293 cells were transfected using Lipofectamine 2000 (Invitrogen) with 2 μg of DNA for each plasmid studied per well. Expression of GFP was used as a marker of positively transfected cells, and recordings were made after 18–36 h.

Electrophysiology—Whole cell recordings were performed as previously described (16, 38). A holding potential of −60 mV was used. Patch electrodes were filled with 140 mM CsCl, 10 mM 1,2-bis-(2-aminophenoxy)-ethane-*N,N,N,N*-tetraacetic acid, 10 mM HEPES (pH 7.4), 4 mM $MgCl_2$, 2 mM ATP, and 0.5 mM GTP. The external solution contained 150 mM NaCl, 10 mM KCl, 2.0 mM $CaCl_2$, 1.0 mM $MgCl_2$, 10 mM HEPES (pH 7.4), and 10 mM glucose. For G protein activation experiments, GTPγS (0.5 mM) was added directly to the internal solution, replacing GTP. The amplitude of the glycine current was assayed using a short (1–2 s) pulse of 30–40 μM glycine every 60 s as previously described (16). Strychnine (1 μM) blocked all of the current elicited by wild type and mutant glycine receptors (not shown).

Construction of Glutathione S-Transferase Fusion Proteins and GST Pull-down Assays—DNA fragments encoding wild type and mutant GlyR intracellular loops were subcloned in the GST fusion vector pGEX-5X3 (GE Healthcare). GST fusion proteins were generated in *Escherichia coli* BL21 using 50 μM isopropyl β-D-thiogalactopyranoside. After 6 h, the cells were collected and sonicated in lysis buffer (1× phosphate buffer, 1% Triton X-100, and protease inhibitor mixture set II (Calbiochem)). Subsequently, the proteins were purified using a glutathione resin (Novagen). Normalized amounts of GST fusion proteins were incubated with purified Gβγ protein (10 ng; Calbiochem). Incubations were done in 800 μl of binding buffer (200 mM NaCl, 10 mM EDTA, 10 mM Tris, pH 7.4, 0.1% Triton X-100, and protease inhibitor mixture set II) at 4 °C for 1 h. The beads were washed five times in binding buffer, and bound proteins were separated on 12% SDS-polyacrylamide gels. Bound Gβγ was detected using a Gβ antibody (1:1000; Santa Cruz Biotechnology) and a chemiluminiscence kit (PerkinElmer Life Sciences). Finally, the relative amounts of Gβγ were quantified by densitometry. Similar conditions have been used to study the interaction between Gβγ and other effector proteins (15, 20–22, 35, 36).

Immunofluorescence, Visualization, and Analysis—HEK 293 cells were first fixed for 30 min with 4% paraformaldehyde (0.1 M phosphate buffer, pH 7.4) and were then permeabilized (0.3% Triton X-100, 30 min) and blocked (10% normal horse serum, 60 min). Subsequently, all night incubation with a monoclonal FLAG (Stratagene) and polyclonal hexahistidine antibodies (His-Tag; U.S. Biological) was carried out. Epitope visualization was performed incubating the sample with two secondary antibodies conjugated to fluorescein isothiocyanate and Cy3 (1:600; Jackson ImmunoResearch Laboratories). Finally, the cells were coverslipped using fluorescence mounting medium (Dako Cytomation; Dako). For quantitative analysis, the cells were chosen randomly for imaging using a Nikon confocal microscopy. Stacks of optical sections in the *z* axis were acquired, and dual color immunofluorescent images were captured in simultaneous two-channel mode. Colocalization was studied by superimposing both color channels. The cross-correlation coefficient (*r*) between both fluorescence channels was measured using computer software (Metamorph; Universal Imaging Corp.) starting from separate immunoreactivity to GlyR-His and Gβ_1-FLAG in the same cell (39). The theoretical maximum for (*r*) is 1 for identical images, and a value close to 0 implies a complete different localization of the labels. Subsequently, the obtained data were compiled, analyzed, and plotted.

Molecular Modeling—The GlyR model was constructed by homology using coordinates from the *Torpedo* nAchR at 4 A° resolution (28, 29) (Protein Data Bank code 2BG9) using the program WHAT IF (40). The ligand-binding segment of the GlyR was modeled from the acetylcholine-binding protein structure (30) (Protein Data Bank code 1UV6). Electrostatic surface potentials were calculated using APBS (41). The individual charges were assigned using pdb2pqr software (42) with the AMBER force field (43). The final images were generated with Pymol (44).

Data Analysis—Statistical analyses were performed using ANOVA and are expressed as the arithmetic means ± S.E.; values of $p < 0.05$ were considered statistically significant. For all of the statistical analysis and plots, the Origin 6.0 (MicroCal) software was used. The normalized values were obtained by dividing the current amplitude obtained with time of dialysis by the current at minute one. The control GTPγS percentage potentiation is the average for all of the single experiments.

RESULTS

Effects of G Protein Activation on Wild Type and Truncated Human α_1 Glycine Receptor Subunits—The currently accepted topology of the LGIC superfamily predicts that the large intracellular loop between transmembrane domains 3 and 4 is the region for interaction and regulation by intracellular pathways, including receptor phosphorylation (10–14). Noteworthy, Ser^{391} was the first residue in this sequence reported to be modulated by phosphorylation by protein kinase C (13). The cytosolic loop polypeptide contains ≈84 amino acids (Fig. 1*A*), which can present alternative splicing. Therefore, we examined the sensitivity of a recently identified α_1 splicing variant, in which the sequence between residues Glu^{326} and Lys^{355} was

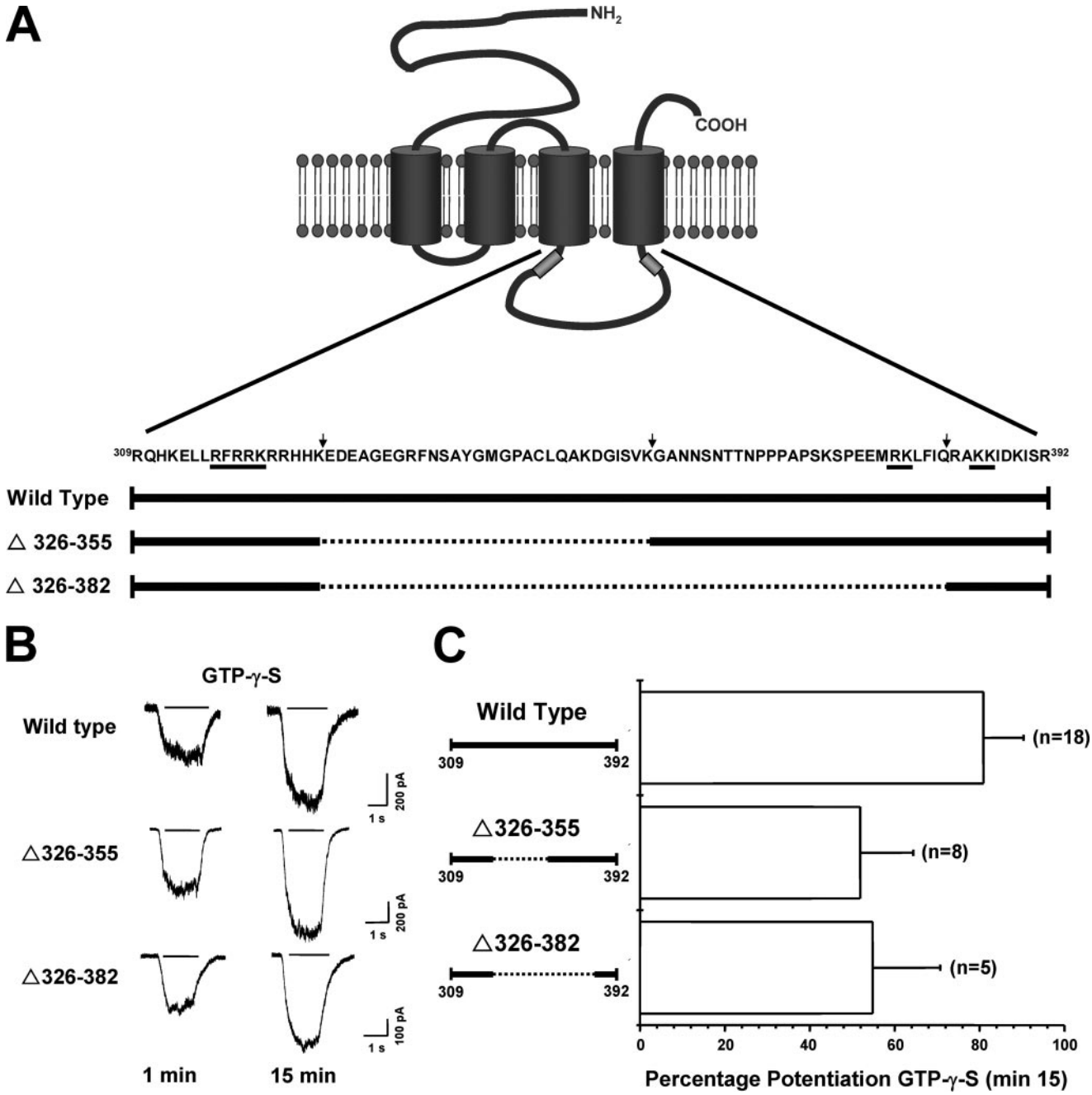

FIGURE 1. **Effects of G protein activation on native and truncated glycine receptors.** *A*, topological model of the GlyR α_1 subunit and primary sequence of TM3-TM4 intracellular loop. The numbers correspond to positions in the mature polypeptide. Truncated sequences are schematized by the *dashed line* and *arrows*. Important modulatory sites are underlined and shown in *light gray* within the cartoon model. *B*, current traces obtained in transfected HEK cells with wild type and truncated forms of GlyRs recorded at 1 and 15 min of whole cell recording using intracellular GTPγS. *C*, the graph summarizes the percentage of potentiation of the glycine current obtained following 15 min of dialysis with GTPγS. Statistical analyses show no significant differences between the constructs.

deleted (24), to Gβγ modulation (Fig. 1*A*). In addition, we constructed a truncated GlyR, in which the whole sequence between residues Glu^{326} and Gln^{382} was deleted (Fig. 1*A*). As previously reported (16), the amplitude of the glycine-activated current in human wild type GlyRs was strongly enhanced above control (80 ± 10%, $n = 18$) after 15 min of intracellular dialysis with GTPγS (Fig. 1, *B* and *C*). Interestingly, similar effects were found on Δ326–355 and Δ326–382 truncated GlyRs (Fig. 1, *B* and *C*), and no statistical differences were detected (Fig. 1*C*). Thus, these data indicate that the whole deleted sequence between residues 326 and 382 is not a critical determinant for Gβγ modulation and directs further analysis toward other regions in the intracellular loop.

Two Basic Motifs Are Critical for G Protein βγ Functional Modulation of Glycine Receptors—Studies on the molecular determinants involved in the binding and modulation by G protein βγ to several proteins have shown the existence of key basic amino acids (19–23). Interestingly, the large intracellular loop of the GlyR has a high density of residues, such as lysine and arginine (23 of 84), with several in a cluster near the transmem-

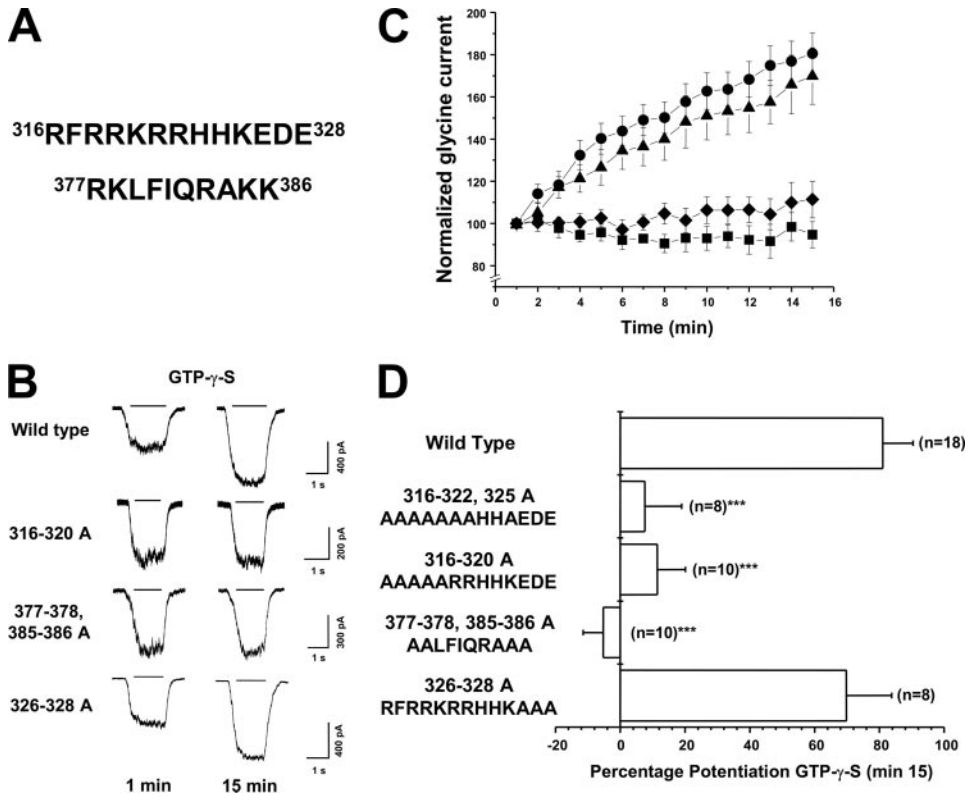

FIGURE 2. **Effects of G protein activation in mutant glycine receptors.** *A*, amino acid sequences of the regions studied. *B*, glycine evoked currents in the presence of intracellular GTPγS in wild type and mutant GlyRs. *C*, time course of GTPγS mediated effects on wild type (*circles*), 316–320A mutant (*diamonds*), 326–328A mutant (*triangles*), and 377–378, 385–386A (*squares*). *D*, the graph summarizes the percentage potentiation of the glycine current obtained following 15 min of dialysis with GTPγS. The *asterisks* denote a significance of $p < 0.05$ (*), $p < 0.01$ (**), or $p < 0.001$ (***); ANOVA. The enhancement of the glycine current in the 326–328A mutant was not different from wild type.

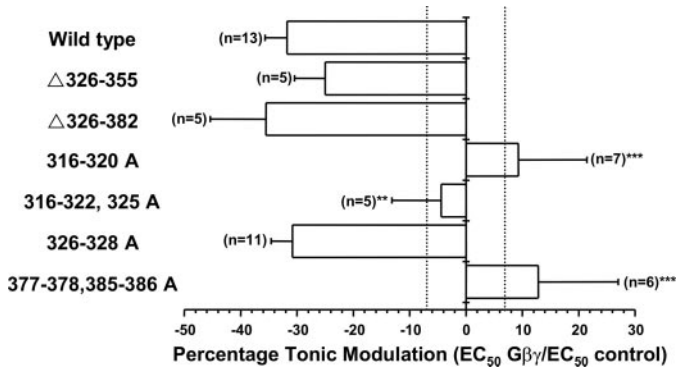

FIGURE 3. **Tonic Gβγ modulation of native and mutant glycine receptors expressed in HEK 293 cells.** The graph illustrates the percentage of tonic modulation obtained in several GlyRs after Gβγ overexpression comparing the glycine concentration response for each condition. A *negative number* indicates a left shift in the glycine dose-response curve. *Dashed lines* represent 2 S.E. of the value for wild type GlyRs. *Asterisks* denote a significant difference between the tonic modulation percentage of the GlyR studied as compared with the wild type (**, $p < 0.01$; ***, $p < 0.001$; ANOVA).

brane domain 3 (TM3), ^{316}RFRRKRR (Fig. 2*A*). This cluster was found to be important for correct membrane topology of GlyRs (25). To investigate the importance of this motif on the G protein modulation, we studied mutant GlyRs in which these basic residues, together with a phenylalanine, were replaced by alanines. The data shows that GTPγS-mediated current enhancement was significantly attenuated in the 316–320A (11 ± 9%, $n = 10$) and the 316–322,325A (8 ± 11%, $n = 8$) mutants (Fig. 2, *B–D*). On the other hand, the data in Fig. 2 (*B–D*) show that mutations in an acidic motif (^{326}EDE) near this basic cluster did not affect the receptor sensitivity to modulation (70 ± 13%, $n = 8$). The finding that GTPγS affected the 316–320A and 316–322,325A mutants in a similar fashion (Fig. 2*D*) suggests that residues 316–320 are the main determinants for Gβγ modulation. Nevertheless, the GlyR intracellular loop has two other pairs of basic residues near the C-terminal (^{377}RK^{385}KK; Figs. 1*A* and 2*A*), and we studied the functional importance of those residues on receptor modulation. Interestingly, the alanine replacement of these four residues also significantly attenuated the effect of G protein activation (−5 ± 7%, $n = 8$), in a similar way to the 316–320A mutant (Fig. 2, *B–D*).

It is known that Gβγ overexpression can induce tonic modulation of Ca^{+2}, GIRK channels, and GlyRs (16, 26, 27). Therefore, we examined the ability of wild and mutant GlyRs to display this phenomenon. In these experiments, the concentration-response relationship for the wild type α_1 GlyRs was shifted to the left after Gβγ dimers were coexpressed, as reflected by a significant reduction in its EC_{50} (−32 ± 4%) with respect to control cells (Fig. 3). Tonic modulation was absent in the 316–320A; 377–378, 385–386A (9 ± 12% and 12 ± 14%, respectively), which is in line with the loss of glycine-activated current potentiation after GTPγS dialysis. Other constructs where the basic residues were retained displayed normal tonic modulation after Gβγ coexpression (Fig. 3). Regarding the cell surface expression of these functional constructs, we found that with the exception of the 316–320A (25), all of the mutants studied displayed very similar maximal current values. For example, the amplitude of the maximal current (I_{max}) elicited by 1 mM glycine was 3339 ± 460 pA ($n = 13$) for the 377–378, 385–386A mutant, which was not significantly different from wild type GlyRs (3647 ± 394 pA, $n = 23$). On the other hand, although the truncated GlyRs showed lower I_{max} relative to wild type (Δ326–382, 1584 ± 210 pA, $n = 11$), the G protein modulation was unchanged. Thus, these data suggest that the elimination of G protein βγ modulation is independent of changes on cell surface expression. Thus, all of the above shows the importance of the basic residues in the functional G protein βγ modulation of GlyRs.

To identify critical amino acids involved in the G protein modulation, we carried out a mutagenesis scanning in these two regions found to be important for modulation. For the ^{316}RFRRK cluster, all single point mutations showed marked

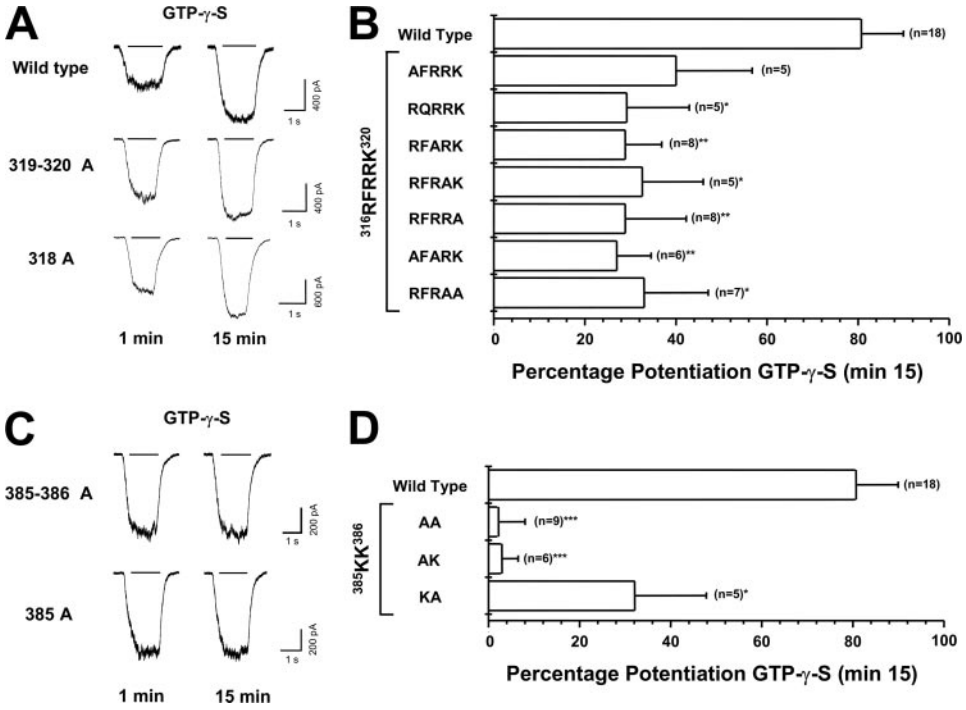

FIGURE 4. **Effects of mutations within the basic motifs on G protein modulation.** *A*, glycine-activated responses to intracellular GTPγS of single and double mutated GlyRs. *B*, the bar graph summarizes the effects of the nonhydrolyzable GTP analog on the glycine evoked current. Differences were significant (*, $p < 0.05$; **, $p < 0.01$; ANOVA). *C*, current traces of single and double mutated GlyRs evoked currents in the presence of intracellular GTPγS. *D*, the graph summarizes the effects of the nonhydrolyzable GTP analog on the glycine evoked current. The differences were significant (*, $p < 0.05$; ***, $p < 0.001$; ANOVA).

attenuations in the potentiating effect produced by the GTP analog, compared with the wild type GlyRs (Fig. 4*A*). For example, the potentiation for R316A was 40 ± 17% ($n = 5$), whereas the effect for K320A was only 29 ± 13% ($n = 8$). Interestingly, the mutation F317Q also altered the modulation (29 ± 14%, $n = 5$) implicating hydrophobic residues, in addition to basic ones, in the modulatory effects. Double mutants RK319–320A and RR316,318A were also less affected than the wild receptor (27 ± 8%, $n = 6$ and 33 ± 14%, $n = 7$, respectively) but were no different from the point mutants (Fig. 4, *A* and *B*). On the other hand, for the basic residues detected near the C-terminal region, no potentiation was detected in the double mutant 385–386A (2 ± 6%, $n = 9$), suggesting a critical role for the ^{385}KK residues (Fig. 4, *C* and *D*). Subsequent studies with the point mutations K385A and K386A showed significant attenuations (3 ± 4%, $n = 6$ and 32 ± 16%, $n = 5$, respectively), confirming an important role for the ^{385}KK motif for this intracellular regulation. Altogether, the data show the main importance of the basic motifs ^{316}RFRRK and ^{385}KK in the Gβγ modulation of GlyRs, suggesting that all of these residues are necessary for the functional effect.

Basic Motifs Are Involved in the Protein Interaction between Gβγ and Glycine Receptor—To determine whether the intracellular motifs identified are necessary for the binding of Gβγ to the GlyR, we constructed GST fusion proteins encoding wild type and mutated forms of the GlyR intracellular loop in which the functional G protein modulation was abolished. GST fusion proteins were first expressed and purified (Fig. 5*A*), and then *in vitro* binding assays were performed using purified Gβγ, under conditions that warrant the native conformation of the heterodimer (15, 17, 18, 20–22, 36). In agreement with the functional data and previous reports for other effectors (15, 19–22, 35, 36), we found that the wild type TM3-TM4 loop was able to bind Gβγ in comparison with GST alone (Fig. 5, *A* and *B*), confirming the direct interaction. The GST-GlyR fusion proteins that contained the 316–320A and 385–386A mutations were also able to bind Gβγ, although to a lower degree as compared with the wild type GlyR sequence (Fig. 5, *A–C*). Therefore, we also tested the capacity of a GST-GlyR construct containing mutations in both functional regions to bind purified Gβγ. Interestingly, when both motifs were mutated, the Gβγ binding to the GlyR intracellular sequence was significantly reduced (Fig. 5, *A–C*). These results indicate that the ^{316}RFRRK and ^{385}KK motifs in the TM3-TM4 loop are directly involved in the Gβγ binding and suggest that each site can independently bind Gβγ in the GST pull-down assay. To further study the functional and biochemical data in a more intact cellular context, we performed a set of double immunofluorescent experiments in HEK 293 cells transfected with mutant and wild type GlyRs with $G\beta_1\gamma_2$ subunits using hexahistidine and FLAG epitopes to identify the expressed GlyRs and $G\beta_1$ subunits, respectively. In agreement with the biochemical and functional tonic modulation data, the cellular distribution of wild type GlyRs and Gβγ dimers displayed a significant overlap in their expression patterns (Fig. 5*D*). Subsequently, we made similar experiments using mutant GlyRs functionally insensitive to G protein modulation. For the 316–320A and 377–378,385–386A mutants, for example, the near cellular association found between wild type GlyRs and Gβγ immunoreactivities was attenuated, showing a reduced degree of colocalization (Fig. 5*D*). To quantify this data, a correlation analysis for the colocalization of both proteins was performed, and the correlation coefficient (r), a quantitative measure of colocalization, was calculated from each cell analyzed. For the wild type GlyRs, correlation analysis yielded a high correlation coefficient value ($r = 0.73 \pm 0.02$, $n = 23$) (Fig. 5*E*), providing quantitative support for a high level of colocalization between wild GlyRs and Gβγ. On the other hand, data with the 316–320A and 377–378,385–386A mutants showed significant lower values ($r = 0.40 \pm 0.05$, $n = 14$; $r = 0.50 \pm 0.03$, $n = 19$; respectively). Although the limit of resolution for laser scanning confocal microscopy is inconclusive in showing an actual physical interaction between proteins, the significant colocalization of GlyR and Gβγ detected is consistent with the idea of direct interaction in the cells, in agreement with the biochemical data obtained using immunoprecipitation (16) and GST pull-down. Altogether, these data demonstrate that the basic residues within

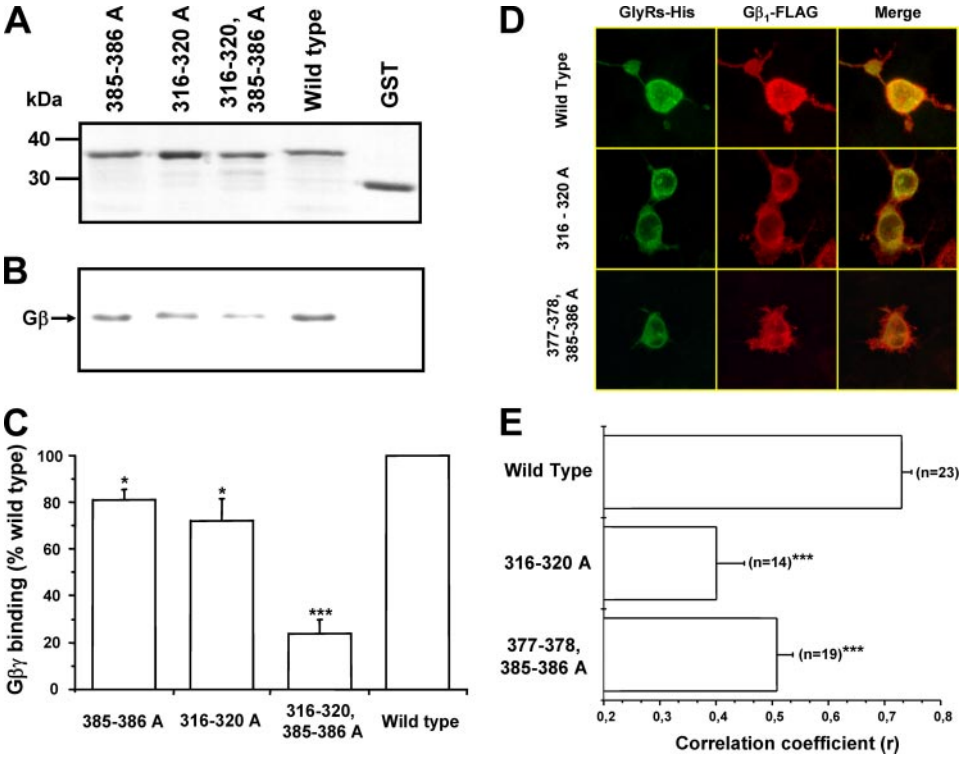

FIGURE 5. **Role of the basic motifs in the protein interaction between Gβγ and GlyRs.** *A*, Coomassie Blue stain for the GST fusion proteins used. *B*, Gβγ binding to wild type and mutant GlyRs. An *arrow* indicates the Gβγ detected with a polyclonal anti-Gβ antibody. *C*, relative amounts of bound Gβγ compared with the wild type intracellular loop ($n = 4$). The differences were significant (*, $p < 0.05$; ***, $p < 0.001$; ANOVA). *D*, transfected HEK 293 cells were stained with antibodies against the hexahistidine (*green*) and FLAG epitopes (*red*) that recognize tagged GlyRs and $G\beta_1$, respectively. The images were merged to visualize colocalization (*yellow*). *E*, the graph summarizes the mean correlation coefficients (*r*) between the wild type and mutant GlyRs with $G\beta_1\gamma_2$ subunits. The differences were significant (***, $p < 0.001$; ANOVA).

DISCUSSION

The GlyR is a member of the ligand-gated ion receptor superfamily, which also includes γ-aminobutyric acid type A receptors, nAChRs, and 5-HT_3 receptors. These homologous ionotropic receptors mediate fast synaptic transmission in the central nervous system. Interestingly, all of the members of the superfamily share common features. For example, all have the signature Cys-loop, a conserved disulfide loop in their extracellular ligand-binding domain, and all are composed of five subunits in a heteropentameric quaternary structure arranged around a central pore. Each subunit possesses a large extracellular domain and four transmembrane α-helixes per subunit with a large intracellular loop between the third and fourth TM. This model was first suggested by hydrophobicity plots of the ligand-gated channels and was recently confirmed by biochemical and crystallographic data from studies with nAChR (2, 28, 29, 32). Coincidentally, several recent studies showed similar channel gating mechanisms for the LGIC members; involving the ligand-binding domain and the extracellular loop between TM2 and TM3 (32–34).

the intracellular loop are involved in the protein interaction and functional modulation between GlyRs and Gβγ.

Localization and Characterization of G Protein βγ Modulatory Sites within the LGIC Member Structure—To study the possible conformation and localization of these motifs in the ion channel, we generated a GlyR α_1 subunit model based on the acetylcholine-binding protein and *Torpedo* nAChR structure coordinates (28–30). In this model, the motifs ^{316}RFRRK and ^{385}KK are cytosolic α-helixes near transmembrane regions 3 and 4, in close proximity to the lipid bilayer and display a high density of positive charges (Fig. 6*A*, shown in *blue*). Additionally, the model also predicts close proximity of these regions in the whole GlyR pentameric structure (Fig. 6*B*). Thus, in the quaternary receptor structure, the Gβγ-binding site can be shaped by positive residue motifs in neighboring subunits in close relationship to the membrane and the receptor vestibule. Additional computer simulations indicated that the regions identified are potentially favorable to interact with the effector-interacting face of Gβγ, in agreement with previous reports (31) (data not shown). Thus, in line with experimental evidence in voltage-gated calcium channels (20), the data allow proposal of a model in which the two regions identified, composed mainly by basic residues at both sides of the cytoplasmic loop of GlyRs, are key regions for appropriate Gβγ binding and functional modulation.

Because of these common receptor properties, it was not surprising to find that the regulation of the LGIC family by intracellular signal transduction pathways is also conserved. Several studies, for example, have demonstrated functional regulation of the LGIC family by protein kinases, involving the phosphorylation of specific residues inside the intracellular loop between TM3 and TM4 (6, 10–14). Besides protein kinases, recent evidence have shown that the activity of two members of the LGIC family (GlyRs and nAchRs) was directly modulated by G protein βγ subunits, enhancing the activity of both channels (15, 16).

For several Gβγ effectors, a large variety of G protein modulatory sites were characterized. Biochemical and functional data studies determined multiple binding and modulatory sites in voltage-gated calcium channels and GIRK channels, indicating a high degree of complexity (19, 20, 23, 35, 36). Despite this, the presence of basic residues inside the critical regions for binding and modulation appears to be a common feature. For example, intracellular arginine residues in different domains of voltage-gated calcium channels have been shown to be critical for binding and regulation by Gβγ (19, 20, 23). Moreover, mutations in basic amino acids decreased the Gβγ binding to β-adrenergic receptor kinase 1 and phos-

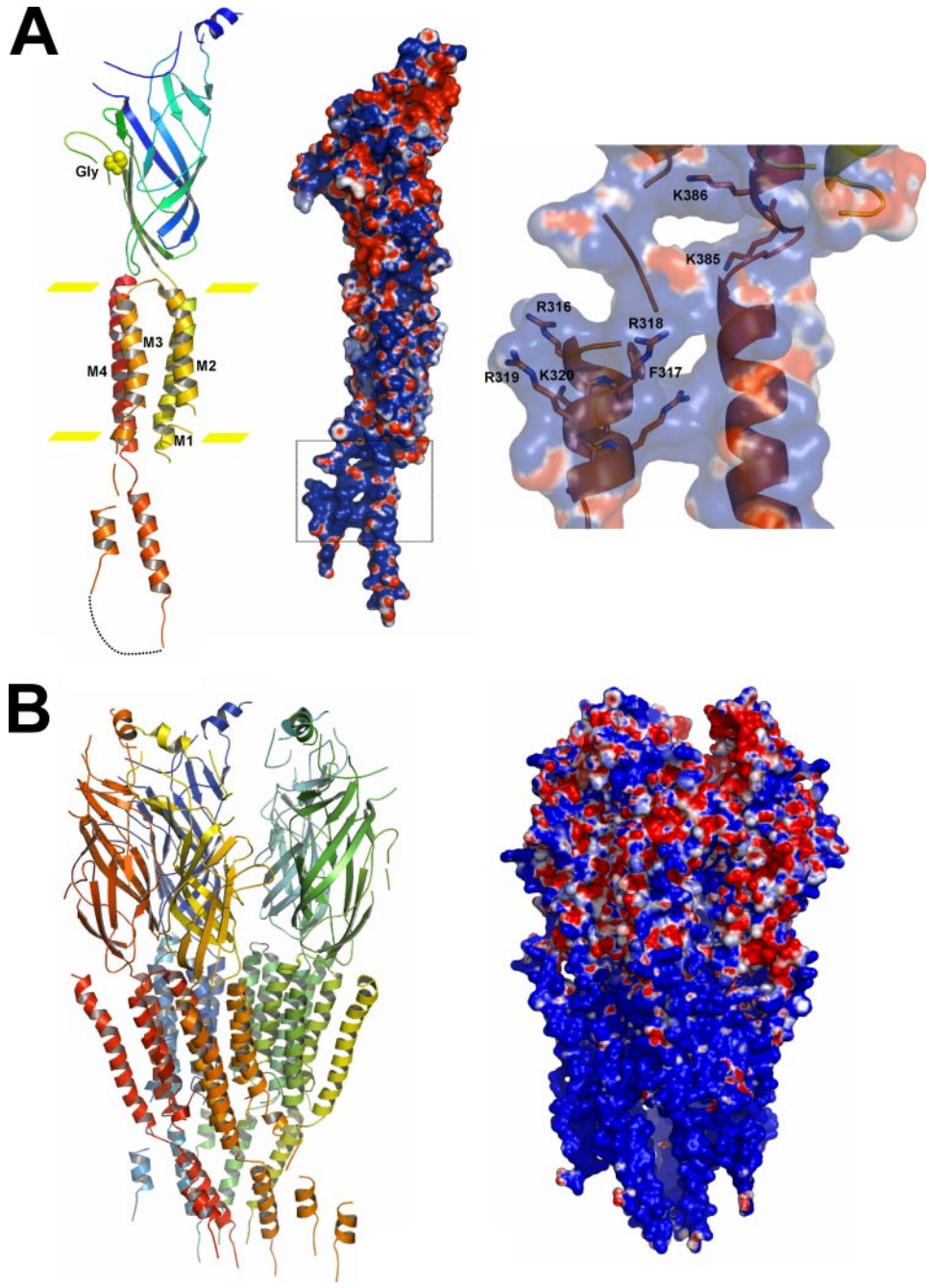

FIGURE 6. **Localization and characterization of the G protein βγ modulatory sites within the GlyR structure.** *A*, ribbon diagram and electrostatic potential surface representations of a single GlyR α_1 subunit derived from the nAChR template. The *right panel* shows a detailed view of the motifs important for Gβγ modulation. Negative and positive charges are in *red* and *blue*, respectively. *B*, ribbon and electrostatic potential surface models of homopentameric GlyRs. In this conformation, the Gβγ modulatory sites of neighboring subunits shape an electropositive surface that serves for binding and functional modulation of channel function.

were located near transmembrane domains 3 and 4, respectively, suggesting a close relationship with the cell membrane. Mutations on either of these sites abolished the functional modulation of GlyRs by G protein activation, supporting critical but independent roles of these regions for functional Gβγ regulation. The GST pull-down assays confirmed a direct interaction between Gβγ and the intracellular loop of α_1 GlyR and indicate that only their concurrent alteration is able to extensively reduce the Gβγ binding. On the other hand, confocal microscopy analysis shows a lower degree of colocalization between Gβγ dimers and mutant forms of GlyRs that includes only one altered motif compared with wild type receptors. This evidence is in agreement with the functional data obtained indicating that both motifs are necessary for a full functional modulation. Besides these observations, our GlyR homology model shows that the motifs identified are cytosolic α-helixes near transmembrane regions 3 and 4, in close proximity to the lipid bilayer and highly electropositive. Interestingly, in a whole GlyR pentameric model both motifs are in close proximity, generating an electropositive surface composed of all of the basic residues of neighboring subunits. Therefore, in line with the experimental evidence, we can postulate that region shapes the membrane-bound Gβγ interaction surface necessary for the functional modulation of GlyRs. Thus, based on this proposal, the alteration of a single basic motif can change this critical interaction surface between pentameric GlyRs and membrane-associated Gβγ.

pholipase Cβ3, affecting the functional modulatory effects (21, 22). However, for GIRK channels no basic residues have been found to be important for Gβγ regulation, indicating vast types of molecular determinants in the heterodimer effects (35, 36).

In our study, using truncated and mutated GlyRs in their intracellular loop, we identify two critical motifs for the Gβγ modulation of α_1 GlyRs. Interestingly, almost all of the amino acids involved were basic, in agreement with most of the data for other Gβγ effectors. The sites ^{316}RFRRK and ^{385}KK

For several Gβγ effectors, a large variety of molecular determinants for binding and modulation have been characterized (17–22, 31, 35, 36). In this study, we provide novel information for the identification of Gβγ modulatory sites in the GlyR, a member of the LGIC superfamily. To our knowledge, we demonstrate a new role for the specific residues in the intracellular loop, in addition to the growing number of critical functions of the LGIC main intracellular loops for correct channel structure, localization, function, and regulation (6, 13, 25, 37).

Acknowledgments—We thank Dr. S. R. Ikeda for plasmids and Lauren Aguayo and Claudia Lopez for technical assistance.

REFERENCES

1. Kandel, E. R., Schwartz, J. H., and Jessell, T. M. (2000) *Principles of Neural Science*, pp. 207–228, McGraw-Hill Book Co., New York
2. Sine, S. M., and Engel, A. G. (2006) *Nature* **440,** 448–455
3. Legendre, P. (2001) *Cell Mol. Life Sci.* **58,** 760–793
4. Aguayo, L. G., van Zundert, B., Tapia, J. C., Carrasco, M. A., and Alvarez, F. J. (2004) *Brain Res. Brain Res. Rev.* **47,** 33–45
5. Laube, B., Maksay, G., Schemm, R., and Betz, H. (2002) *Trends Pharmacol. Sci.* **23,** 519–527
6. Harvey, R. J., Depner, U. B., Wassle, H., Ahmadi, S., Heindl, C., Reinold, H., Smart, T. G., Harvey, K., Schutz, B., Abo-Salem, O. M., Zimmer, A., Poisbeau, P., Welzl, H., Wolfer, D. P., Betz, H., Zeilhofer, H. U., and Muller, U. (2004) *Science* **304,** 884–887
7. Sebe, J. Y., van Brederode, J. F., and Berger, A. J. (2006) *J. Neurophysiol.* **96,** 391–403
8. Harris, R. A. (1999) *Alcohol Clin. Exp. Res.* **23,** 1563–1570
9. Smart, T. G., Hosie, A. M., and Miller, P. S. (2004) *Neuroscientist* **10,** 432–442
10. Smart, T. G. (1997) *Curr. Opin. Neurobiol.* **7,** 358–367
11. Song, Y., and Huang, L. Y. (1990) *Nature* **348,** 242–245
12. Vaello, M. L., Ruiz-Gomez, A., Lerma, J., and Mayor, F. (1994) *J. Biol. Chem.* **269,** 2002–2008
13. Ruiz-Gomez, A., Vaello, M. L., Valdivieso, F., and Mayor, F. (1991) *J. Biol. Chem.* **266,** 559–566
14. Guo, X., and Wecker, L. (2002) *J. Neurochem.* **82,** 439–447
15. Fischer, H., Liu, D. M., Lee, A., Harries, J. C., and Adams, D. J. (2005) *J. Neurosci.* **25,** 3571–3577
16. Yevenes, G. E., Peoples, R. W., Tapia, J. C., Parodi, J., Soto, X., Olate, J., and Aguayo, L. G. (2003) *Nat. Neurosci.* **6,** 819–824
17. Clapham, D. E., and Neer, E. J. (1997) *Annu. Rev. Pharmacol. Toxicol.* **37,** 167–203
18. Hamm, H. E. (1998) *J. Biol. Chem.* **273,** 669–672
19. Dolphin, A. C. (2003) *Pharmacol. Rev.* **55,** 607–627
20. De Waard, M., Liu, H., Walker, D., Scott, V. E., Gurnett, C. A., and Campbell, K. P. (1997) *Nature* **385,** 446–450
21. Barr, A. J., Ali, H., Haribabu, B., Snyderman, R., and Smrcka, A. V. (2000) *Biochemistry* **39,** 1800–1806
22. Touhara, K., Koch, W. J., Hawes, B. E., and Lefkowitz, R. J. (1995) *J. Biol. Chem.* **270,** 17000–170005
23. Canti, C., Page, K. M., Stephens, G. J., and Dolphin, A. C. (1999) *J. Neurosci.* **19,** 6855–6864
24. Inoue, K., Ueno, S., Yamada, J., and Fukuda, A. (2005) *Biochem. Biophys. Res. Commun.* **327,** 300–305
25. Sadtler, S., Laube, B., Lashub, A., Nicke, A., Betz, H., and Schmalzing, G. (2003) *J. Biol. Chem.* **278,** 16782–16790
26. Ikeda, S. R. (1996) *Nature* **380,** 255–258
27. Ruiz-Velasco, V., and Ikeda, S. R. (2001) *J. Physiol.* **537,** 679–692
28. Miyazawa, A., Fujiyoshi, Y., and Unwin, N. (2003) *Nature* **423,** 949–955
29. Unwin N. (2005) *J. Mol. Biol.* **346,** 967–989
30. Celie, P. H., van Rossum-Fikkert, S. E., van Dijk, W. J., Brejc, K., Smit, A. B., and Sixma, T. K. (2004) *Neuron* **41,** 907–914
31. Ford, C. E., Skiba, N. P., Bae, H., Daaka, Y., Reuveny, E., Shekter, L. R., Rosal, R., Weng, G., Yang, C. S., Iyengar, R., Miller, R. J., Jan, L. Y., Lefkowitz, R. J., and Hamm, H.E. (1998) *Science* **280,** 1271–1274
32. Cascio, M. (2004) *J. Biol. Chem.* **279,** 19383–19386
33. Absalom, N. L., Lewis, T. M., Kaplan, W., Pierce, K. D., and Schofield, P. R. (2003) *J. Biol. Chem.* **278,** 50151–50157
34. Kash, T. L., Jenkins, A., Kelley, J. C., Trudell, J. R., and Harrison, N. L. (2003) *Nature* **421,** 272–275
35. He, C., Yan, X., Zhang, H., Mirshahi, T., Jin, T., Huang, A., and Logothetis, D. E. (2002) *J. Biol. Chem.* **277,** 6088–6096
36. Huang, C. L., Slesinger, P. A., Casey, P. J., Jan, Y. N., and Jan, L. Y. (1995) *Neuron* **15,** 1133–1143
37. Kelley, S. P., Dunlop, J. I., Kirkness, E. F., Lambert, J. J., and Peters, J. A. (2003) *Nature* **424,** 321–324
38. Van Zundert, B., Alvarez, F. J., Tapia, J. C., Yeh, H. H., Diaz, E., and Aguayo, L. G. (2004) *J. Neurophysiol.* **91,** 1036–1049
39. Agnati, L. F., Fuxe, K., Torvinen, M., Genedani, S., Franco, R., Watson, S., Nussdorfer, G. G., Leo, G., and Guidolin, D. (2005) *J. Histochem. Cytochem.* **53,** 941–953
40. Vriend, G. (1990) *J. Mol. Graph.* **8,** 52–56
41. Baker, N. A., Sept, D., Joseph, S., Holst, M. J., and McCammon, J. A. (2001) *Proc. Natl. Acad. Sci. U. S. A.* **98,** 10037–10041
42. Dolinsky, T. J., Nielsen, J. E., McCammon, J. A., and Baker, N. A. (2004) *Nucleic Acids Res.* **32,** W665–W667
43. Cornell, W. D., Cieplak, P., Bayly, C. I., Gould, I. R., Merz, K. M., Ferguson, D. M., Spellmeyer, D. C., Fox, T., Caldwell, J. W., and Kollman, P. (1995) *J. Am. Chem. Soc.* **117,** 5179–5197
44. DeLano, W. L. (2002) *The PyMOL Molecular Graphics System*, DeLano Scientific, San Carlos, CA

Molecular Determinants for G Protein βγ Modulation of Ionotropic Glycine Receptors

Gonzalo E. Yevenes, Gustavo Moraga-Cid, Leonardo Guzmán, Svenja Haeger, Laerte Oliveira, Juan Olate, Günther Schmalzing and Luis G. Aguayo

J. Biol. Chem. 2006, 281:39300-39307.
doi: 10.1074/jbc.M608272200 originally published online October 12, 2006
